J. Cent. South Univ. (2014) 21: 1142−1147
DOI: 10.1007/s11771-014-2047-8

Springer

Three-dimensional stability analysis of anisotropic and non-homogeneous slopes using limit analysis

HAN Chang-yu(韩长玉), CHEN Jin-jian(陈锦剑), XIA Xiao-he(夏小和), WANG Jian-hua(王建华)

Department of Civil Engineering, Shanghai Jiaotong University, Shanghai 200240, China

© Central South University Press and Springer-Verlag Berlin Heidelberg 2014

Abstract: A method of three-dimensional loaded slope stability for anisotropic and nonhomogeneous slopes was presented based on the upper-bound theorem of the limit analysis approach. The approach can be considered as a modification and extension of the solutions. The influences of friction angle, anisotropy factor, nonhomogeneous factor, slope angle, ratio of width to depth, and load on the slope crest were investigated. The results show that solutions are suitable to deal with the purely cohesive soils and frictional/cohesive soils, isotropic and anisotropic, homogeneous and nonhomogeneous, loaded and unloaded cases.

Key words: stability; anisotropy; limit analysis; loaded slope; nonhomogeneous slope

1 Introduction

Estimating the slope stability remains an important area of study for geotechnical engineering both in theory and practice. Numerous types of analysis have been proposed for assessing the stability of slopes. In general, these methods can be classified into the following types: the limit equilibrium method [1], the finite element method [2−4] and the limit analysis method [5−9].

Limit analysis, based on plasticity limit theorems, has an advantage of the lower and upper bound theorems to bracket the true solution. This method has been employed to deal with the 2D and 3D slope stability problems. Based on the upper bound limit analysis theorem, ZHAO et al [10] used the equation for expressing critical limit-equilibrium state to define the safety factor of a given slope and its corresponding critical failure mechanism by means of the kinematical approach of limit analysis theory. GANJIAN et al [11] introduced a new rotational collapse mechanism and quasi-static coefficient concept to investigate the influences of soil dilatancy angle on 3D seismic stability of locally-loaded slopes in non-associated flow rule materials.

MICHALOWSKI and DRESCHER [12] introduced a rigorous 3D analysis in the strict framework of a limit analysis of plasticity. In their analysis, the geometry of the slip surface was curvilinear cone and both cohesive and frictional soils were included, which is very powerful, but limited to homogeneous and unloaded slopes. This work is essentially an extension of the work by MICHALOWSKI and DRESCHER [12], in which the proposed upper bound limit analysis formulation is the same. In this work, different anisotropy and nonhomogeneous factors are included in order to analyze the stability of loaded slopes.

2 Limit analysis theorems

Limit analysis is a powerful mathematical tool that provides rigorous lower and upper bounds to the exact stability factor in slope stability problems. The soil is assumed to deform plastically according to the normality rule associated with the Coulomb yield condition. The kinematic approach based on the plasticity upper bound theory has been widely adopted to investigate the problems of slope stability [13−14], ultimate bearing capacity [15], and slurry trench stability [16−17]. The kinematic theorem of limit analysis states that the rate of internal work is not less than the work rate of body force. This can be expressed by the following equation as [18]

$$\int_V \sigma_{ij}^* \dot{\varepsilon}_{ij}^* \mathrm{d}V \geq \int_S T_i v_i \mathrm{d}S + \int_V X_i v_i^* \mathrm{d}V \tag{1}$$

where $\dot{\varepsilon}_{ij}^*$ is strain rate; σ_{ij}^* is stress; S and V are loaded boundary and volume, respectively. The first term is the rate of work done by stress σ_{ij}^* over the virtual strain rate $\dot{\varepsilon}_{ij}^*$, dissipated within V. The second term is the rate of work done by surface forces T_i. The last term on the

Foundation item: Projects(41002095, 41172251, 41272317) supported by the National Natural Science Foundation of China
Received date: 2012−08−20; **Accepted date:** 2013−03−01
Corresponding author: WANG Jian-hua, Professor, PhD; Tel: +86−21−62932915; E-mail: jhwang417@163.com

right-hand side is the work rate of body force X_i. The details of the application of this method to slope stability problems can be found in Ref. [18].

3 Formulation

A 3D rotational mechanism for frictional/cohesive soil with logarithm helicoids surface is shown in Fig. 1, in which the failure surface is assumed to pass through the top and the toe of the slope. The same shape of this mechanism is considered by MICHALOWSKI and DRESCHER [12] for evaluating the stability factor of homogeneous and unloaded slope. Soil over the failure surface rotates about the center of rotation O, while the materials below the failure surface are static. Failure surface AC is a velocity discontinuous surface. A more comprehensive description and discussion of this mechanism can be found in Ref. [12].

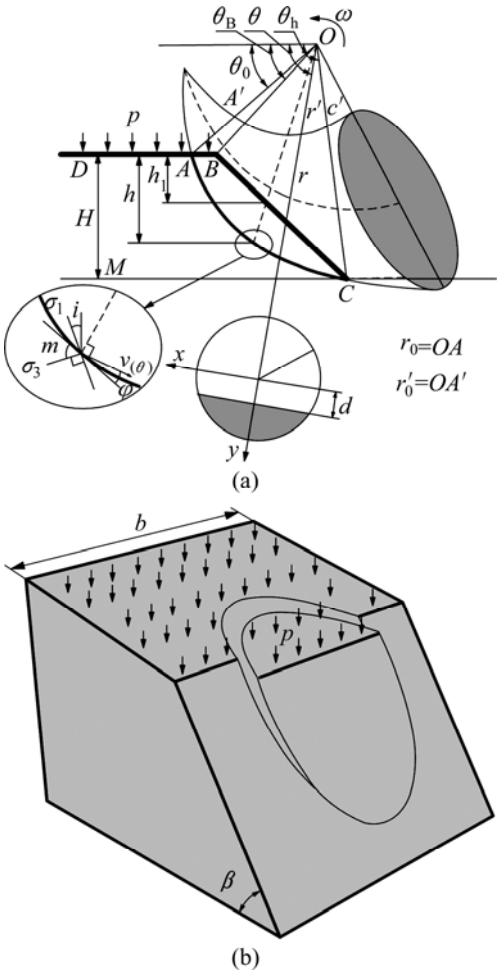

Fig. 1 Schematic diagram of 3D mechanism

The rate of work of the external forces (weight) is

$$W_\gamma = 2\omega\gamma[\int_{\theta_0}^{\theta_B}\int_0^{x_1^*}\int_a^{y^*}(r_m+y)^2\cos\theta\,dy\,dx\,d\theta + \int_{\theta_B}^{\theta_h}\int_0^{x_2^*}\int_d^{y^*}(r_m+y)^2\cos\theta\,dy\,dx\,d\theta] \quad (2)$$

where γ is the unit weight of the soil, and ω is the angular velocity. The two integrals relate to the work rate in the upper portion of the slope in the range (θ_0, θ_B), and in the remaining part of the slope (θ_B, θ_h).

The rate of energy dissipated along the discontinuity surface is

$$D = 2\omega[\int_{\theta_0}^{\theta_B}\int_a^R \frac{c_i R(r_m+y)^2}{\sqrt{R^2-y^2}}dy\,d\theta + \int_{\theta_B}^{\theta_h}\int_d^R \frac{c_i R(r_m+y)^2}{\sqrt{R^2-y^2}}dy\,d\theta] \quad (3)$$

where

$$r_m = \frac{r+r'}{2}, R = \frac{r-r'}{2} \quad (4)$$

$$x_1^* = \sqrt{R^2-a^2}, x_2^* = \sqrt{R^2-d^2}, y^* = \sqrt{R^2-x^2} \quad (5)$$

$$a = \frac{\sin\theta_0}{\sin\theta}r_0 - r_m, d = \frac{\sin(\beta+\theta_h)}{\sin(\beta+\theta)}r_0 e^{(\theta_h-\theta_0)\tan\varphi} - r_m \quad (6)$$

$$\theta_B = \arctan\frac{\sin\theta_0\sin\beta}{\sin(\theta_h+\beta)e^{(\theta_h-\theta_0)\tan\varphi} - \sin\theta_0\cos\beta} \quad (7)$$

$$r = r_0 e^{(\theta-\theta_0)\tan\varphi}, r' = r_0' e^{-(\theta-\theta_0)\tan\varphi} \quad (8)$$

The load (p) velocity during rotation about axis O is

$$v_p = \frac{\sin\theta_0}{\sin\theta}r_0\omega \quad (9)$$

The rate of external work due to the load on the slope crest is

$$W_p = 2\omega r_0^2\sin^2\theta_0\int_{\theta_0}^{\theta_B} p\frac{\cos\theta}{\sin^3\theta}\sqrt{R^2-a^2}\,d\theta \quad (10)$$

In this work, it is assumed that only the cohesive strength is nonhomogeneous and anisotropic. A very common case of nonhomogeneity of cohesion is that of a linear variation of C_h with respect to depth z as shown diagrammatically in Fig. 2 [19−20]. The cohesion C_h is the horizontal cohesive strength. The ratio of relative

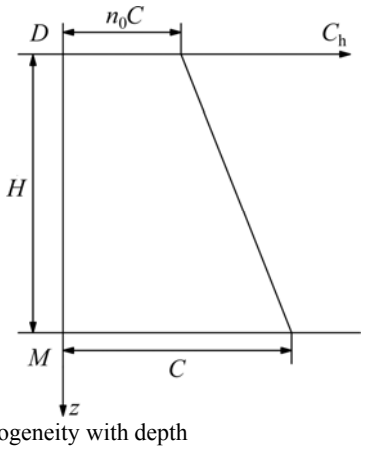

Fig. 2 Nonhomogeneity with depth

cohesions at the level of the top (n_0C) and toe (C) is defined by n_0.

According to the geometric relationship in Fig. 2, the cohesive strength C_{h1} at the vertical symmetry plane of the mechanism can be expressed as

$$C_{h1} = C[n_0 + \frac{h}{H}(1-n_0)] \tag{11}$$

where the parameters h and H are obtained from the geometrical and trigonometric relations in Fig. 1 as

$$h = r\sin\theta - r_0\sin\theta_0 = r_0[\sin\theta e^{(\theta-\theta_0)\tan\varphi} - \sin\theta_0] \tag{12}$$

$$H = r_0[\sin\theta_h e^{(\theta_h-\theta_0)\tan\varphi} - \sin\theta_0] \tag{13}$$

The cohesive strength $C_{h'}$ at the slope face can be expressed as

$$C_{h'} = \frac{h_1}{H}C + \frac{H-h_1}{H}n_0C \tag{14}$$

where h_1 is derived from geometrical relations in Fig. 1 as

$$h_1 = r_x\sin\theta - r_0\sin\theta_0 \tag{15}$$

where r_x is the distance from the rotation center to the slope face as

$$r_x = \frac{\sin(\beta+\theta_h)}{\sin(\beta+\theta)}r_0 e^{(\theta_h-\theta_0)\tan\varphi} \tag{16}$$

The cohesion C_h along any cross-sectional plane of the mechanism in Fig. 1 can be expressed as

$$C_h = \frac{y-a}{R-a}C_{h1} + \frac{R-y}{R-a}n_0C,\ \ \theta_0 \le \theta \le \theta_B \tag{17}$$

$$C_h = \frac{y-d}{R-d}C_{h1} + \frac{R-y}{R-d}C_{h'},\ \ \theta_B \le \theta \le \theta_h \tag{18}$$

It is assumed that the variation of cohesion with direction approximates to the curve, as shown in Fig. 3 [19−20]. The cohesion C_i at the place where the major principal stress direction inclines at an angle i to the vertical direction is given as

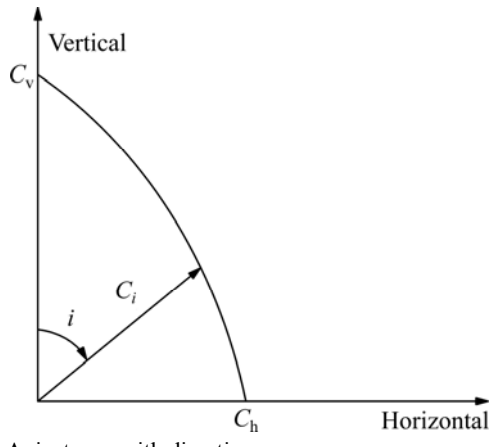

Fig. 3 Anisotropy with direction

$$C_i = C_h + (C_v - C_h)\cos^2 i = C_h(1 + \frac{1-k}{k}\cos^2 i) \tag{19}$$

where k is the ratio of the principal cohesions c_h/c_v.

Equating the total rates of external works Eqs. (2) and (10) to the total rates of internal energy dissipation Eq. (3), it is obtained

$$\frac{\gamma H}{C} = f(\theta_0, \theta_h, r_0'/r_0) \tag{20}$$

The function $f(\theta_0, \theta_h, r_0'/r_0)$ has a minimum and thus indicates a least upper bound when θ_0, θ_h and r_0'/r_0 satisfy the conditions:

$$\frac{\partial F}{\partial\theta_0} = 0,\quad \frac{\partial F}{\partial\theta_h} = 0,\quad \frac{\partial F}{\partial(r_0'/r_0)} = 0 \tag{21}$$

The corresponding values for θ_0, θ_h and r_0'/r_0 satisfying Eq. (21) result in $N_s = \min[f(\theta_0, \theta_h, r_0'/r_0)]$. Thus, the critical height (H_c) can be expressed as

$$H_c \le \frac{C}{\gamma}N_s \tag{22}$$

The estimates of stability factor $\gamma H/C$ are obtained using a minimization procedure for given friction angle (φ), slope angle (β), ratio of width to depth (B/H), anisotropy factor (k), nonhomogeneous factor (n_0) and load on the slope crest ($p/\gamma H$). Independent variables in the minimization procedure are angles θ_0 and θ_h, and ratio r_0'/r_0. These parameters are varied by a small increment in computational loops, and the process is repeated until the minimum of $\gamma H/C$ is reached, with the increments of 0.001° used for angles θ_0 and θ_h, and 0.001 for ratio r_0'/r_0.

4 Comparison with 2D results

CHEN [20] introduced a rigorous 2D analysis in the strict framework of a limit analysis of plasticity. In the analysis, the geometry of the slip surface was logspiral, unloaded and nonhomogeneous slopes were included. In this section, 2D solutions for various parameters are compared accroding to CHEN's work, including φ, n_0, k and β. For the 3D slopes, it is usually considered that with an increase in width (B), the safety factor approaches the one from 2D analysis. In order to facilitate the comparison of 2D and 3D calculations, B/H=2 is taken in 3D cases. The results of these computations are graphically represented in Figs. 4−7.

Figure 4 illustrates the effect of friction angle (φ) on the stability factor. As expected, the stability factor increases as φ increases. It can be found that increasing φ from 20° to 30° can increase the stability factor by more than 27%. Figure 5 presents the influence of the slope

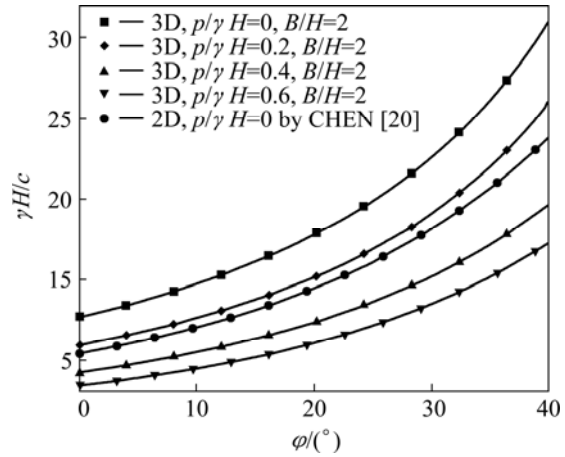

Fig. 4 Comparison of results with different φ for n_0=0.7, k=0.7 and β=70°

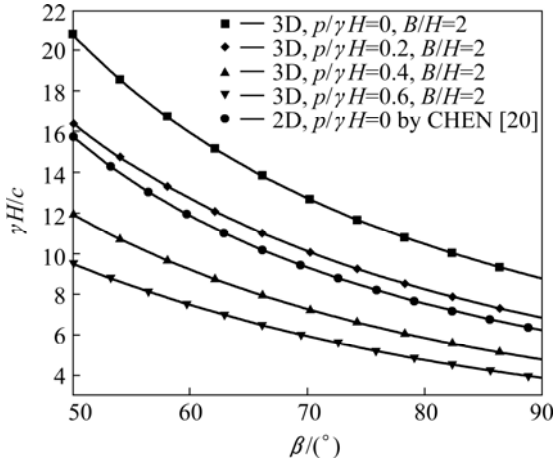

Fig. 5 Comparison of results with different β for φ=20°, n_0=0.7 and k=0.7

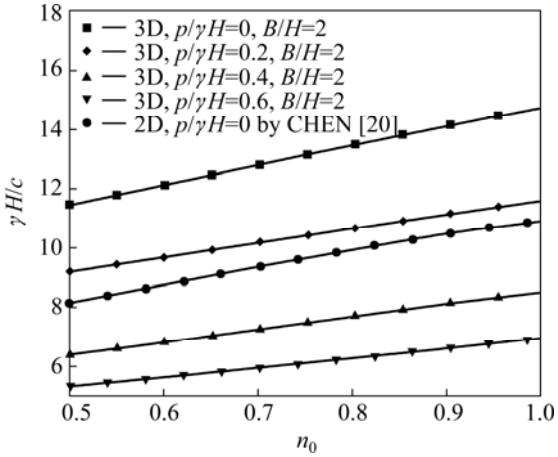

Fig. 6 Comparison of results with different n_0 for φ=20°, k=0.7 and β=70°

angle (β) on the stability factor. The results indicate that increasing β from 60° to 80° can decrease the stability factor by 34%. Figure 6 shows the relation between the stability factor and the nonhomogeneous factor (n_0) for different soil properties, and the line marked with filled

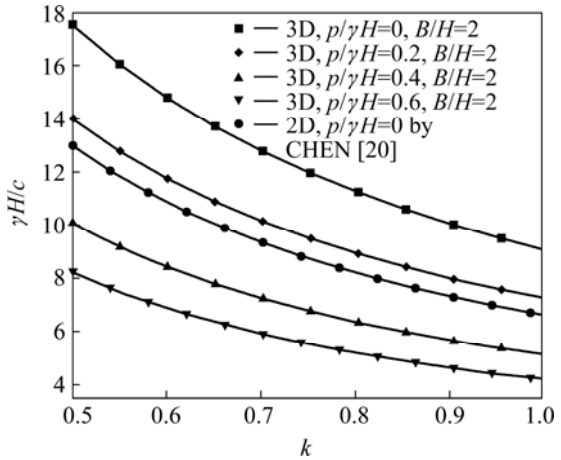

Fig. 7 Comparison of results with different k for φ=20°, n_0=0.7 and β=70°

dot indicated the 2D results [20]. It is observed that increasing n_0 from 0.6 to 0.8 can increase the stability factor by 10%. Figure 7 displays that the stability factor varies when the anisotropy factor (k) is changed. It can be seen that increasing k from 0.6 to 0.8 can decrease the stability factor by more than 24%.

Referring to Figs. 4−7, the stability factor for the 3D results (B/H=2 and $p/\gamma H$=0) are around 1.51 times larger than the stability factor of the 2D results ($p/\gamma H$=0). The difference in 3D and 2D stability factor of slopes can be measured by the vertical distance between the respective lines in these figures. The stability factor from a 3D analysis will approach the stability factor from a 2D analysis gradually when the ratio of width to depth increases.

5 Comparison with other 3D results

In this section, the results in this work are compared to Michalowski's 3D solutions for purely cohesive and frictional/cohesive slopes. Figures 8 and 9 show comparison of stability factors for the isotropic (k=1) and anisotropic ($k\neq1$), homogeneous (n_0=1) and non-homogeneous ($n_0\neq1$), loaded ($p/\gamma H\neq0$) and unloaded ($p/\gamma H$=0) cases.

Figures 8 and 9 also illustrate the effect of ratio of width to depth (B/H) on the stability factor in 3D cases. From these figures, the ratio of width to depth, B/H, is found to have large effect on the stability factor when B/H<3. It can be found that increasing B/H from 1 to 3 can decrease the stability factor by more than 18%. This means that the 3D boundary effect is very large when B/H<3. From the observation of Figs. 8 and 9, the range of this difference changes less than 2%, when the ratio of B/H increases from 5 to 10. This implies that the 3D boundary end effect on slope stability is small and almost insignificant when $B/H\geq5$.

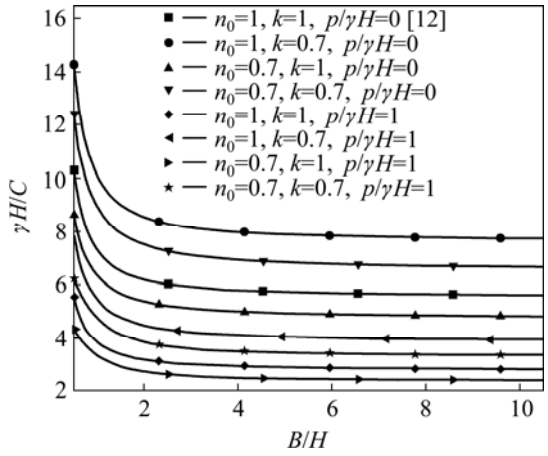

Fig. 8 Comparison of results with different B/H for φ=0° and β=70°

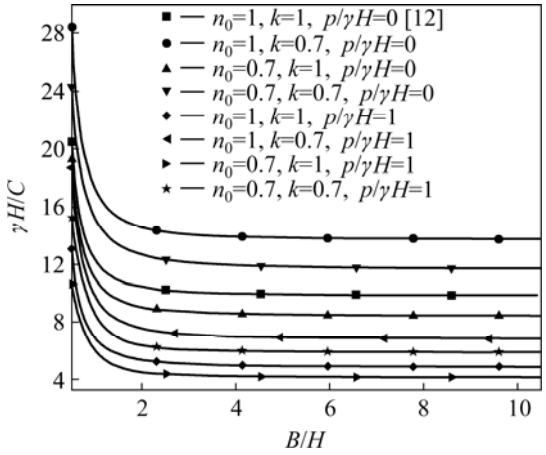

Fig. 9 Comparison of results with different B/H for φ=0° and β=70°

6 Effects of load on slope crest

Figure 10 illustrates a variation of the stability factor with $p/\gamma H$ for n_0=0.7, k=0.7 and φ=20°. As expected, the stability factor decreases as $p/\gamma H$ increases. It can be seen from Fig. 10 that increasing $p/\gamma H$ from 0 to 0.5 can decrease the stability factor by more than 47%.

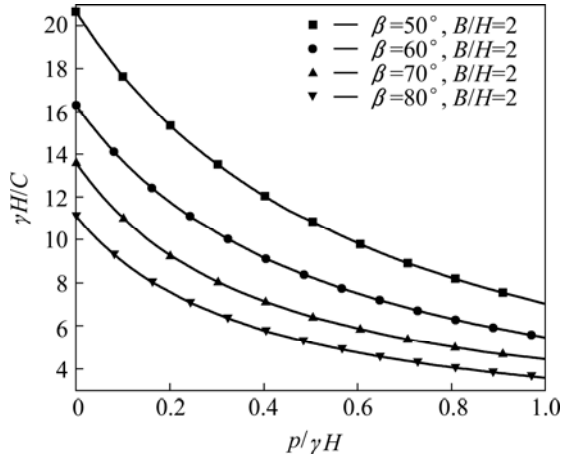

Fig. 10 Effect of load in critical height of slope for n_0=0.7, k=0.7 and φ=20°

7 Conclusions

1) Based on the upper-bound theorem of limit analysis, the 3D loaded slope stability analysis for anisotropic and nonhomogeneous slopes is presented. The stability analysis for uniform soil slopes is modified and extended to anisotropic, nonhomogeneous and loaded slopes.

2) Examples are provided to illustrate variations of the stability factor with friction angle, anisotropy factor, nonhomogeneous factor, slope angle, ratio of width to depth, and load on the slope crest. The stability factor increases with increasing friction angle, non-homogeneous factor, and with decreasing slope angle, anisotropy factor, ratio of width to depth, and load on the slope crest.

3) The solutions are suitable to deal with the following cases, purely cohesive soils and frictional/cohesive soils, isotropic and anisotropic, homogeneous and nonhomogeneous, loaded and unloaded.

References

[1] ZHENG H. A three-dimensional rigorous method for stability analysis of landslides [J]. Engineering Geology, 2012, 145: 30−40.

[2] ZHANG F M, WANG B H, CHEN Z Y, et al. Rock bridge slice element method in slope stability analysis based on multi-scale geological structure mapping [J]. Journal of Central South University of Technology, 2008, 15: 131−137.

[3] LIN H, CAO P, GONG F Q, et al. Directly searching method for slip plane and its influential factors based on critical state of slope [J]. Journal of Central South University of Technology, 2009, 16(1): 131−135.

[4] CHEN S H, WANG W M, ZHENG H F, et al. Block element method for the seismic stability of rock slopes [J]. Journal of Geotechnical and Geoenvironmental Engineering, 2010, 136(12): 1610−1617.

[5] CHEN Z Y, SUN P, WANG Y J, et al. 3-dimensional slope stability analyses using non-associative stress-strain relationships [J]. Science in China Series E-Technological Sciences, 2009, 52(9): 2517−2527.

[6] SUN G H, ZHENG H, JIANG W. A global procedure for evaluating stability of three-dimensional slopes [J]. Natural Hazards, 2012, 61(3): 1083−1098.

[7] YANG X L, HUANG F. Slope stability analysis considering joined influences of nonlinearity and dilation [J]. Journal of Central South University of Technology, 2009, 16(2): 292−296.

[8] GAO Y, ZHANG F, LEI G, LI D Y. An extended limit analysis of three-dimensional slope stability [J]. Geotechnique, 2013, 63(6): 518−524.

[9] GAO Y, ZHANG F, LEI G, et al. Stability charts for 3D failures of homogeneous slopes [J]. Journal of Geotechnical and Geoenvironmental Engineering, 2012. doi: 10.1061/(ASCE) GT.1943−5606.0000866.

[10] ZHAO L H, LI L A, YANG F, et al. Upper bound analysis of slope stability with nonlinear failure criterion based on strength reduction technique [J]. Journal of Central South University of Technology,

2010, 17(4): 836−844.

[11] GANJIAN N, ASKARI F, FARZANEH O. Influences of nonassociated flow rules on three-dimensional seismic stability of loaded slopes [J]. Journal of Central South University of Technology, 2010, 17(3): 603−611.

[12] MICHALOWSKI R L, DRESCHER A. Three-dimensional stability of slopes and excavations [J]. Geotechnique, 2009, 59(10): 839−850.

[13] XIA X H, HAN C Y, WANG J H. Analytical solutions for three-dimensional stability of limited slopes [J]. Journal of Shanghai Jiaotong University (Science), 2012, 17(2): 251−256.

[14] HAN C Y, XIA X H, WANG J H. Analytical solutions for three-dimensional stability of coastal slope. In New Frontiers in Engineering Geology and the Environment, Huang, Y.,Wu, F.,Shi, Z., etc., Eds. Springer Berlin Heidelberg: 2013, 9: 181−185.

[15] HAN C Y, XIA X H, WANG J H. Upper bound solutions of ultimate bearing capacity of curved footing [J]. Chinese Journal of Geotechnical Engineering, 2012, 34(2): 230−236. (in Chinese)

[16] HAN C, WANG J, XIA X, et al. Limit analysis for local and overall stability of slurry trench in cohesive soil [J]. International Journal of Geomechanics, 2012. doi:10.1061/(ASCE)GM.1943−5622.0000268.

[17] HAN C Y, CHEN J J, WANG J H, et al. 2D and 3D stability analysis of slurry trench in frictional/cohesive soil [J]. Journal of Zhejiang University-Science, 2013, 14(2): 94−100.

[18] MICHALOWSKI R L. Stability of uniformly reinforced slopes [J]. Journal of Geotechnical and Geoenvironmental Engineering, 1997, 123(6): 546−556.

[19] NIAN T K, CHEN G Q, LUAN M T, et al. Limit analysis of the stability of slopes reinforced with piles against landslide in nonhomogeneous and anisotropic soils [J]. Canadian Geotechnical Journal, 2008, 45(8): 1092−1103.

[20] CHEN W F. Limit analysis and soil plasticity [M]. Amsterdam: Elsevier, 1975: 399−445.

(Edited by FANG Jing-hua)